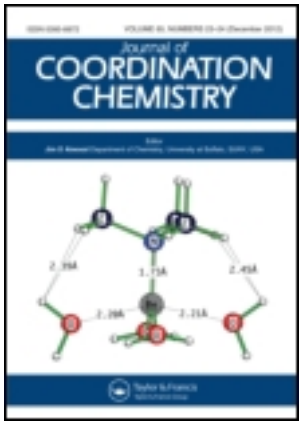

Journal of Coordination Chemistry
Publication details, including instructions for authors and subscription information:
http://www.tandfonline.com/loi/gcoo20

The stabilities and formation kinetics of some macrocycles with copper(II): crystal structures of some pendant arm macrocycles

Hava Ozay [a] , Yakup Baran [a] & Hiroshi Miyamae [b]

[a] Department of Chemistry, Art and Science Faculty , Onsekiz Mart University , Canakkale 17100 , Turkey

[b] Department of Chemistry , Josai University , Keyakidai 1-1, Sakado , Saitama 350-0295 , Japan

Published online: 20 Apr 2011.

To cite this article: Hava Ozay , Yakup Baran & Hiroshi Miyamae (2011) The stabilities and formation kinetics of some macrocycles with copper(II): crystal structures of some pendant arm macrocycles, Journal of Coordination Chemistry, 64:8, 1469-1480, DOI: 10.1080/00958972.2011.574128

To link to this article: http://dx.doi.org/10.1080/00958972.2011.574128

Journal of Coordination Chemistry
Vol. 64, No. 8, 20 April 2011, 1469–1480

The stabilities and formation kinetics of some macrocycles with copper(II): crystal structures of some pendant arm macrocycles

HAVA OZAY†, YAKUP BARAN*† and HIROSHI MIYAMAE‡

†Department of Chemistry, Art and Science Faculty,
Onsekiz Mart University, Canakkale 17100, Turkey
‡Department of Chemistry, Josai University, Keyakidai 1-1,
Sakado, Saityama 350-0295, Japan

(*Received 31 August 2010; in final form 25 February 2011*)

Kinetics of complex formation and stability constants of tetra-(2-hydroxpropyl) substituted cyclam (L^3) and cyclen (L^4) with copper(II) have been studied in aqueous solution at room temperature. These data are compared to the corresponding parent compounds (cyclam L^1 and cyclen L^2) in an attempt to define the effect of pendant arm upon kinetics and stability constants of the complexes. The kinetics were observed by stopped-flow measurements followed at multiwavelengths. These ligands were chosen to furnish information concerning effect of pendant groups and cavity size on the kinetics and stability of the complexes. Stopped-flow and spectrophotometric titration techniques were used for evaluation of the kinetics and stability constants, respectively. The apparent rate constants increase as $CuL^3 > CuL^4 > CuL^1 > CuL^2$. Activation parameters and stability constants of the complexes were estimated. The effect of cavity size on the rate of reaction can be observed in $CuL^3 > CuL^4$ and $CuL^1 > CuL^2$ and the effect of pendant groups in $CuL^3 > CuL^1$ and $CuL^4 > CuL^2$. Mechanism of the complex formation reaction is proposed. The enhanced stability of the copper(II) complexes formed with L^1 and L^2 macrocyclic ligands is compared to those formed with analogous pendant arm species.

Keywords: Kinetics; Stability; Pendant arm; Cavity size; Stopped-flow; Spectroscopic titration

1. Introduction

Macrocycles are polydentate ligands containing their donor atom either incorporated in or attached to a cyclic backbone. Coordination chemistry of macrocyclic compounds has undergone spectacular growth, largely due to the synthesis of a great number and variety of synthetic macrocycles which coordinate to metals. Macrocycles are resistant to degradation, have high thermal stability and are stable in strong acids and bases. They have high kinetic and thermodynamic stability associated with metal ion macrocyclic complexes. The reason for the increased stability is believed to be a

*Corresponding author. Email: yakupbaran@yahoo.com

ISSN 0095-8972 print/ISSN 1029-0389 online © 2011 Taylor & Francis
DOI: 10.1080/00958972.2011.574128

macrocyclic effect which is the extension of the chelate effect. Macrocyclic complexes offer greater stability than the corresponding open chained multidentate ligands by approximately 10^4. The chelate effect partially explains the difference but does not explain such a large difference. Apart from the range of macrocycles that exist based on just the size of the ring and the number of donors, the ability to append side arms to the macrocycle can also change both the structure and functionality of the macrocycles. Pendant arms can be attached directly to the donor atoms which can affect the nature of its metal ion coordination [1]. Pendant arms may consist of flexible components such as alkyl chain containing any number of functional groups including amines, alcohols, amides and carboxyl or aromatic groups with other additional donors [2–8]. The stability of macrocyclic complex is affected by a number of structural characteristics. Therefore, it is possible to design macrocycles that fit better with one metal ion than another, making it possible for the macrocycle to selectively bind one metal over another. The closer the fit between the metal ion and the size of the cavity, the better the fit, thus higher the stability of the complex. This provides the opportunity to develop specific metal ion sensors by manipulating the structure of macrocycles [7–11]. Macrocycles are found throughout nature, a reason for the great interest they have aroused. Vitamin B_{12} coenzyme is a naturally occurring organometallic compound incorporating a cobalt–carbon bond in its structure [12]. Another is chlorophyll, which is known for its role in initiating photosynthesis in green plants. Macrocycles can be used as models for the biologically important compounds and ion transport [13, 14] and can stabilize unusual oxidation state of transition metal ions. This has led to research exploring the redox behavior of transition metal macrocycles [15, 16]. Tetraazamacrocycles with pendant groups have a history of intense study and continue to draw attention due to their potential use in a broad range of applications in catalysis [17, 18], magnetic resonance imaging [19], antiviral agent [20], radiopharmaceuticals [21, 22], industry, and medicine [23, 24]. Kinetic studies often provide valuable insights into important processes, such as the rate of drug decomposition [25] or the rate of metal ion remediation in heavy metal waste water treatments [26].

The work in this article is focused on the kinetics of complex formation and thermodynamic stability of the complexes as well as synthesis and characterization of the compounds. The complex formation kinetics of copper(II) with pendant arm tetraazamacrocycles L^3 and L^4 and their parent compounds were studied. Structures of the ligands are given in figure 1. Pendant arm macrocycles are characterized by spectroscopic methods and X-ray crystallography. The kinetic and thermodynamic properties of these complexes are reported.

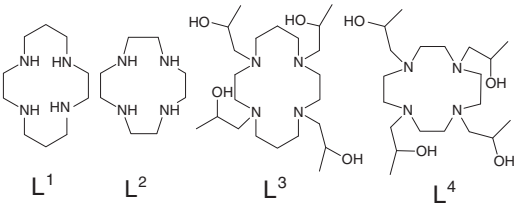

Figure 1. Structures of the ligands.

2. Experimental

2.1. *Materials and measurements*

All commercially available chemicals are of reagent grade and used as received. Ultra pure water which is saturated with argon is used during all spectroscopic studies. Mass spectra are measured with a GC–MS, Thermo Finnigan Trace DSQ. NMR spectra were measured with a Varian 300 MHz spectrometer. Reaction kinetics and spectrophotometric titration are measured with a UV-Vis, Agilent 8453 Diode Array Spectrophotometer and the Pro-K 2000 stopped-flow accessory with pneumatic drive system (applied photophysics) for rapid kinetics studies. For the spectrophotometric titration, acid or base solution is added to solution in 1 cm quartz cell with a peristaltic pump (Cole Palmer, Masterflex) and pH of the solution was measured with an Orion pH meter combined with a Metrohm semi-micro electrode. Temperature was controlled with re-circulated water bath in both cell holder and stopped-flow accessory with the sensitivity ± 0.1°C. Stock solutions were stored at -10°C until needed. FT-IR spectra were measured with a Perkin Elmer BXII spectrometer. Elemental analyses were performed on a LOCO, CHNO element analyzer. Magnetic measurements were accomplished on a MSB MK1 instrument (Sherwood Scientific Ltd.) at ambient temperature.

2.2. *Synthesis of the ligands*

2.2.1. Preparation of 1,4,8,11-tetra(2-hydroxypropyl)-1,4,8,11-tetraazacyclotetradecane, L^3. Propylene oxide (1.71 mL, 30 mmol) was added to a solution of cyclam (0.80 g, 4 mmol) in ethanol (15 mL) at 25°C on a magnetic stirrer for 20 h. Solvent volume was reduced by rotary evaporation and solution left for crystallization. Clear colorless crystals formed and were washed with ice-cold water (2 mL) and dried under vacuum. Yield 1.12 g, 64%. m.p.: 187–189°C. Found: C, 56.7; H, 11.3; and N, 12.1. Calcd for $C_{22}H_{48}N_4O_4.2H_2O$: C, 56.4; H, 11.2; and N, 11.9. The NMR spectrum (D_2O) ^{13}C: 60.91 (4C), 53.14 (4C), 52.82 (4C), 51.33 (4C), 23.13 (2C), 22.11 (4C), m/z: 433 (M^+), FT-IR (ATR, cm^{-1}): ν(OH): 3414, 3245 sh.

2.2.2. Preparation of 1,4,7,10-tetra(2-hydroxypropyl)-1,4,7,10-tetraazacyclotetradecane, L^4. Propylene oxide (1.71 mL, 30 mmol) was added to a solution of cyclen (1.27 g, 4 mmol) in water (15 mL) at 25°C on a magnetic stirrer for 24 h at room temperature. Solvent volume was reduced by rotary evaporation and solution left for crystallization. Clear colorless crystals formed and were washed with ice-cold water (2 mL) and dried under vacuum. Yield 0.95 g, 59%. m.p.: 177–179°C. Found: C, 59.7; H, 11.1; and N, 13.7. Calcd for $C_{20}H_{40}N_4O_4$: C, 59.4; H, 10.9; and N, 13.8. The NMR spectrum (D_2O) ^{13}C: 60.7 (4C), 53.51 (4), 52.71 (8C), 21.82 (4), m/z: 404 (M^+), FT-IR (ATR, cm^{-1}): ν(OH): 3414, 3280 sh.

2.3. *Preparation of the complexes*

General procedure: A stirred solution of macrocycle (1 eq) in a methanol/water mixture (5 : 1) was added to a round-bottomed flask fitted with a water-cooled condenser.

Copper(II) perchlorate (1 eq) was added and the reaction mixture was heated to 50°C for 30 min. A purple solution was diluted and absorbed onto a SP Sephedex C-25 cation exchange resin (Na^+ form) and eluted with 0.2 M of $NaClO_4$ solution. The purple band was collected and the eluate volume was reduced by rotary evaporation. The dark purple solution was left at room temperature and solid was filtered and dried in a vacuum oven.

2.4. *Copper(II) complexes of L^3*

Using a general procedure, CuL^3 was prepared from 1,4,8,11-tetra(2-hydroxypropyl)-1,4,8,11-tetraazacyclotetradecane (39 mg, 90 mmol) and (33 mg, 90 mmol) copper perchlorate as blue crystals (55 mg, 88%); m.p.: 244–246°C; Selected FT-IR (ATR, cm^{-1}): 3554, 3235, 2985, 1621, 1440, 1108, and 1075. Analytical data for $C_{22}H_{50}C_{l2}CuN_4O_{12}$: Calcd: C, 37.90; H, 7.23; N, 8.04. Found: C, 37.78; H, 7.48; and N, 8.11.

2.5. *Copper(II) complexes of L^4*

Using a general procedure, CuL^4 was prepared from 1,4,7,10-tetra(2-hydroxypropyl)-1,4,7,10-tetraazacyclododecane (36 mg, 90 mmol) and (33 mg, 90 mmol) copper perchlorate as blue crystals (46 mg, 81%); m.p.: 235–237°C; Selected FT-IR (ATR, cm^{-1}): 3571, 3248, 2981, 1632, 1438, 1078, 1013. Analytical data for $C_{20}H_{46}C_{l2}CuN_4O_{12}$: Calculated: C, 35.90; H, 6.93; N, 8.37. Found: C, 35.78; H, 6.48; and N, 8.51.

2.6. *Magnetic susceptibility*

The magnetic characteristics of complexes were 1.68 BM for CuL^3 and 1.77 for CuL^4, indicative of the presence of Cu^{2+} with one unpaired electron, close to the spin only value for mononuclear copper(II) complexes.

2.7. *Electronic spectra*

UV-Vis spectrum of copper(II) complexes of pendant arm macrocycles in water exhibited the intense metal-to-ligand charge transfer band around 310 nm and a broad and weak band at 500–600 nm (table 1; figure 2) assigned to *d–d* transitions.

2.8. *Kinetics*

The complex formation kinetics of the copper(II) complexes ($Cu(ClO_4)_2$ was used) with L^1, L^2 and pendant arms of these L^3 and L^4 were studied in acetic acid–acetate buffer solutions (pH = 4.5). Variation of the second order rate constants with pH for CuL^2 complex formation is given in figure 3. Kinetic runs were followed under second order conditions with 1.2 mmol ligand and metal concentrations; $\ln(k/T)$ *versus* $1/T$ graph for CuL^3 is given in figure 4. For activation parameters, kinetic runs were followed at four different temperatures in aqueous solution with the combination of an Agilent HP 8453

Table 1. λ_{max} and colors of the complexes at 298K.

		UV-Vis	
Complex (color)	pH	(λ_{max}, nm)	ε/((mol L^{-1})$^{-1}$cm^{-1})
CuL^1 (purple)	5.04	313 (1845)	546(322)
CuL^2 (purple–blue)	5.00	320 (1345)	565(412)
CuL^3 (blue)	5.02	324 (1390)	577(380)
CuL^4 (blue)	5.03	315 (1750)	590(418)

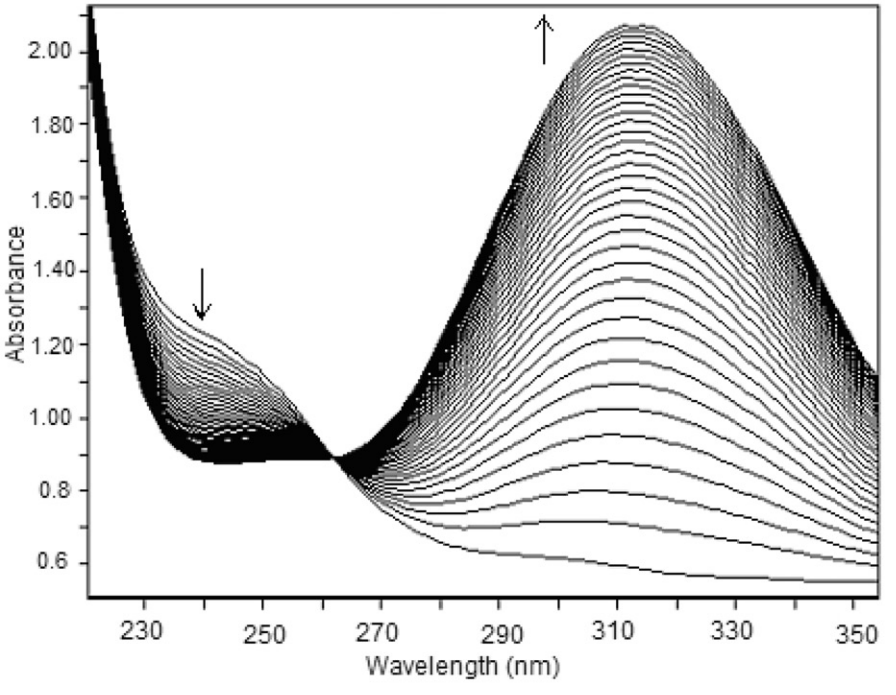

Figure 2. 2-D spectral changes during complex formation of CuL^4 at pH = 5.04, μ = 0.1 M $NaClO_4$, [M] = [L] = 1.20 mmol.

Diode Array UV-Vis spectrophotometer and a Pro-K 2000 rapid kinetics system with pneumatic drive system. Global kinetic analysis and Specfit/32 software were used for kinetic data analysis. Measurements were made at multiwavelengths, and kinetic traces are acquired at all the wavelengths. For the copper(II) kinetics study, argon saturated, deionized, ultra pure water was used. Each kinetic run was repeated at least three times. Ionic strength of the solutions was adjusted to 0.1 M $NaClO_4$. Rate constants and activation parameters are given in table 2.

2.9. *Spectrophotometric titrations*

Stability constants of the complexes were measured with an automatic titration setup, consisting of a computer interfaced to an Agilent HP 8453 Diode Array

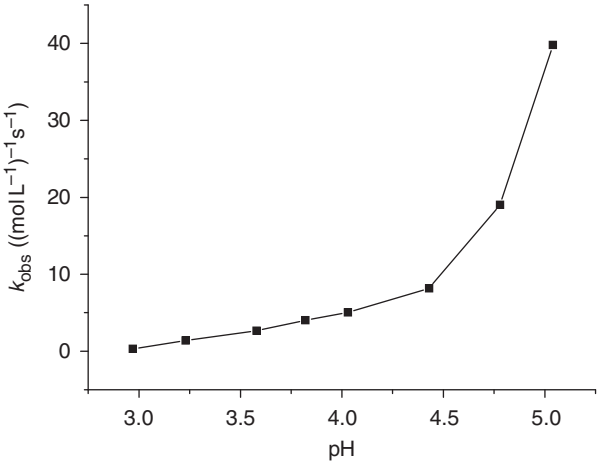

Figure 3. Variation of the second order rate constants for complexation of CuL^2 in aqueous solution over a wide range of pH. The resulting second order rate constants show strong dependence on the pH of solution. Buffer solutions: (chloroacetic acid–acetate) at 298 K.

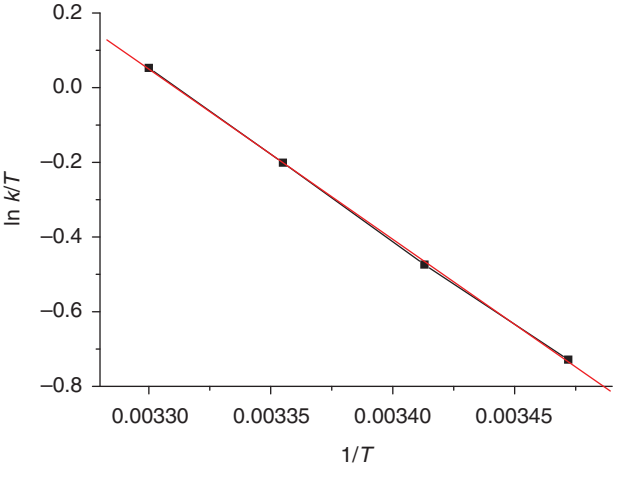

Figure 4. $\ln(k\,T^{-1})$ *vs.* $1/T$ graph for CuL^3.

Spectrophotometer with a stirrer under thermostated cell holder, a peristaltic pump (Cole Palmer, Masterflex) and an Orion pH meter combined with a Metrohm semi-micro electrode. Electrode was calibrated with pH 4 and 7 buffers for measurements in aqueous solutions. Argon saturated aqueous solution of ligand (1.2 mmol) containing 0.1 M of $NaClO_4$ for adjustment of ionic strength was titrated with 10 µL of 0.1 M NaOH at 60 s intervals in a 1 cm quartz cell which was thermostated to $25 \pm 0.1^{\circ}C$ during titration. The cell contains a pH electrode and a capillary tip from the peristaltic pump. Data analysis was carried out using the nonlinear least-square fitting program of Specfit/32. An initial guess for the equilibrium constant was entered and iteratively refined until the best fit was achieved, which was indicated by least squares. Stability constants of the complexes are given in table 3.

Table 2. Rate constants and activation parameters for complex formation at 25°C and I = 0.1 M $NaClO_4$.

Complex	pH	k ($(mol\,L^{-1})^{-1}\,s^{-1}$)	$\Delta H^{\neq}$ ($kJ\,mol^{-1}$)	$\Delta S^{\neq}$ ($J\,K^{-1}\,mol$)
CuL^1	5.01	39.81 ± 0.08	68	10
CuL^2	5.00	2.58 ± 0.08	90	63
CuL^3	5.02	243.71 ± 0.81	38	71
CuL^4	5.03	70.47 ± 0.04	54	53

Table 3. Stability constants of the complexes at 20°C, $\mu = 0.1$ M $NaClO_4$.

Ligand	Metal	M, L, H	$\log \beta_{MLH}$	Equilibrium, K	$\log K_{MLH}$
L^1	Cu^{+2}	110	27.23	$M + L \rightleftarrows ML$	27.23 ± 0.07
		111	33.19	$ML + H \rightleftarrows MLH$	5.96 ± 0.08
L^2	Cu^{+2}	110	25.65	$M + L \rightleftarrows ML$	25.65 ± 0.03
		111	29.62	$ML + H \rightleftarrows MLH$	3.97 ± 0.09
L^3	Cu^{+2}	110	24.34	$M + L \rightleftarrows ML$	24.34 ± 0.05
		111	29.12	$ML + H \rightleftarrows MLH$	4.7 ± 0.07
L^4	Cu^{+2}	110	22.55	$M + L \rightleftarrows ML$	22.55 ± 0.04
		111	26.53	$ML + H \rightleftarrows MLH$	3.98 ± 0.08

2.10. *Crystal structure determinations*

Colorless crystals of L^3 and L^4, suitable for structure determination were obtained from methanol by controlled slow effusion. The X-ray data were collected at −150°C on a Rigaku Mercury CCD area detector with graphite monochromated Mo-Kα ($\lambda = 0.7107$ Å). Data were collected and processed using CrystalClear, Rigaku [27]. The structure was solved by direct methods [28] and expanded using Fourier techniques [29]. The non-hydrogen atoms were refined anisotropically. Some hydrogens were refined isotropically and the rest were refined using the riding model. Structures were solved by direct methods and refined by full-matrix least-squares on F^2 using the SIR92 program. Details of the crystal parameters, data collection, and refinements for L^3 and L^4 are summarized in table 4. Selected bond lengths and angles for L^3 and L^4 are listed in table 5.

2.11. *Ligand L^3 and L^4*

The relevant crystal data and refinement details are given in section 2. L^3 and L^4 crystallized as colorless prisms in methanol in the monoclinic, $P2_1/n$ and $I2/a$ space groups, respectively. The structures consist of discrete centro-symmetric molecules. ORTEP drawing of the molecules is shown in figure 5. A detailed listing of bond lengths and angles has been deposited as supporting information. The crystal structure of the free ligand, L^4, shows that the pendant 2-hydroxypropyl groups are not equivalent. Two are folded over the macrocycle and maintained by intramolecular hydrogen bonds involving an O–H and neighboring tertiary amine of the cyclen ring while the others were extended and pointed away to minimize steric congestion. Intramolecular hydrogen bond seemed to be irregular with a longer O–H bond length than usual. The C–O bond length changed between 1.338 and 1.412 Å. There were four

Table 4. Crystallographic data, data collection procedure, structure determination, and refinement for L^3 and L^4.

	L^3	L^4
Empirical formula	$C_{22}H_{48}O_4N_4$	$C_{20}H_{44}O_4N_4$
Formula weight (M)	432.65	404.59
Temperature (K)	272	272
Wavelength (Mo-Kα, Å)	0.7107	0.7107
Crystal system	Monoclinic	Monoclinic
Space group	$P2_1/n$	$I2/a$
Unit cell dimensions (Å, °)		
a	10.744(5)	15.81(1)
b	9.474(5)	9.330(6)
c	12.638(7)	16.867(9)
β	97.43(2)	108.59(3)
Volume (Å^3)	1275(1)	2358(2)
Z	2	4
Absorption coefficient (mm^{-1})	8	8
Calculated density (g cm^{-3})	1.126	1.128
F(000)	480.00	880.00
Crystal size (mm^3)	0.30 × 0.30 × 0.10	0.70 × 0.60 × 0.10
θ Range for data collection (°)	3.2–27.5	1.71–30.93
Limiting indices (*h*, *k*, *l*)	$13 \le h \le -13$; $12 \le k \le -11$; $16 \le l \le -16$	$20 \le h \le -20$; $12 \le k \le -12$; $12 \le l \le -21$
Reflection collected	12,621	22,339
Reflections unique/*R*(int)	3687 [$R_{(int)} = 0.078$]	2693 [$R_{(int)} = 0.056$]
Completeness to *θ*	27.46	27.49
Data/restraints/parameters	3687/0/170	2693/0/147
Absorption correction	Multiscan	Multiscan
Min. and max. transmission	0.72 and 0.67	0.51 and 0.34
Refinement method	Full-matrix least-squares on F^2	Full-matrix least-squares on F^2
H atom refinement	Riding model	Riding model
Final *R* indices [$I > 2\sigma(I)$]	$R_1$0.062	$R_1 = 0.0747$
R indices (all data)	$R_1$0.064	$R_1 = 0.0876$
Goodness-of-fit	1.029	0.977
Largest difference peak and hole (e Å^{-3})	0.72 and −0.67	0.47 and −0.25

intramolecular hydrogen bonds in L^3 with bond lengths O1–H···N1: 2.306, O2–H···N2: 2.858 Å O′1–H···N′1: 2.306, O′2-H···N′2: 2.858 Å involving a hydroxyl hydrogen and a neighboring tertiary amine of the cyclam ring. These hydrogen bonding interactions have a significant effect on the conformation of macrocycles.

3. Results and discussion

3.1. *Kinetics*

Since the discovery of the macrocyclic effect, much research has been devoted to the elucidation of the mechanism of ligand complexation with metals. The complex formation kinetics of the pendant arm tetraazamacrocycles have been studied with the labile copper(II). It has been generally accepted that a step-wise mechanism is followed, in which the nitrogens of the cyclic ligand coordinate to the metal center one at a time, with concomitant desolvation of the metal center [30]. Formation of macrocyclic

Table 5. Selected bond lengths (Å) and angles (°) for L^3 and L^4.

L^3		L^4	
Bonds	Distance	Bonds	Distance
O(1)–C(7)	1.427(4)	O(1)–C(6)	1.329(4)
N(1)–C(6)	1.462(2)	N(1)–C(1)	1.475(4)
N(1)–C(5)	1.442(2)	N(1)–C(5)	1.450(4)
N(2)–C(4)	1.463(2)	N(2)–C(3)	1.462(4)
N(2)–C(9)	1.489(2)	O(2)–C(9)	1.420(5)
O(2)–C(10)	1.142(2)	N(2)–C(2)	1.473(5)
L^3		L^4	
	Angles		Angles
O(1)–C(7)–C(8)	107.4(2)	O(1)–C(6)–C(7)	116.5(5)
N(1)–C(5)–C(6)	113.3(1)	O(1)–C(6)–C(5)	122.5(5)
N(1)–C(6)–C(7)	109.9(2)	C(6)–C(5)–N(1)	114.6(3)
O(1)–C(7)–C(8)	107.4(2)	N(1)–C(1)–C(2)	109.7(2)
C(6)–C(7)–C(8)	113.9(4)	C(2)–N(2)–C(8)	110.1(3)
N(1)–C(5)–C(4)	115.3(1)	C(1)–C(2)–N(2)	111.5(2)
O(2)–C(10)–C(9)	129.4(2)	N(2)–C(8)–C(9)	113.6(3)
O(2)–C(10)–C(11)	113.1(2)	C(8)–C(9)–O(2)	110.8(2)
C(9)–N(2)–C(4)	109.3(1)	O(2)–C(9)–C(10)	106.7(3)

complexes has been described as consisting of two major kinetic pathways, k_1 and k_2, where k_1 is the second order rate constant corresponding to the fast formation of intermediate species and k_2 is a first order rate constant corresponding to the slow rearrangement of the intermediate species to its most favored configuration.

$$Cu^{2+} + L \underset{}{\overset{k_1((\text{mol}\,L^{-1})^{-1}\,S^{-1})}{\rightleftharpoons}} [CuL]_{int} \xrightarrow{k_2(s^{-1})} [CuL]^{2+}$$

Under most conditions, the reaction scheme reduces to one kinetically observable second order reaction:

$$Cu^{2+} + L \xrightarrow{k_f} [CuL]^{2+}$$

The initial step is a second order reaction between metal ion and ligand with a formation constant k_1. The resultant intermediate then reacts through a first order reaction to form the final product. Stopped-flow kinetic measurements enabled unraveling the formation process of the copper(II) complexes that proceeds in a single rate-limiting step while the apparent rate constants increase $CuL^3 > CuL^4 > CuL^1 > CuL^2$ as a consequence of the pendant groups in the macrocycles. The cavity of the cyclen and tetrapendant derivative of this ligand are too small to encapsulate copper(II) while that of cyclam and its tetrapendant derivative have enough cavity to include copper(II). The reason behind the different kinetic behavior between the copper complexes of L^1, L^3 and L^2, L^4 seems to be more related to the differences in the structure of the free ligands than in the structure of the copper(II) complexes. As a result, cyclam and tetrapendant analog react much faster than cyclen and tetrapendant analog. In the structure of free L^3, four pendant arms have an anticonfiguration in relation to the plane formed by four nitrogens of the macrocycle. Two are folded over

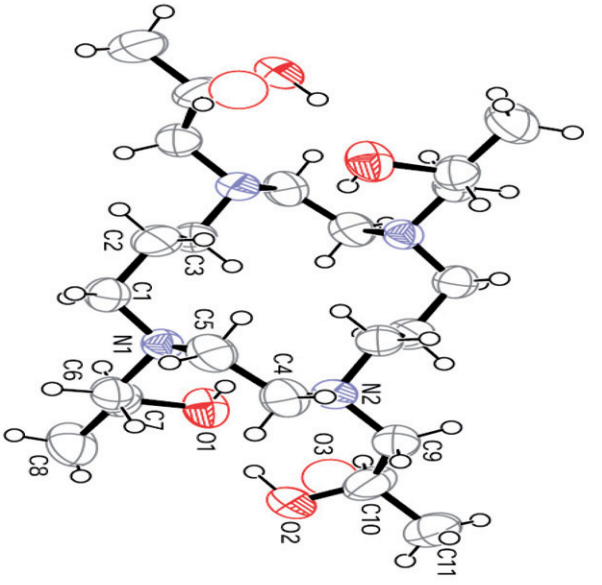

L^3

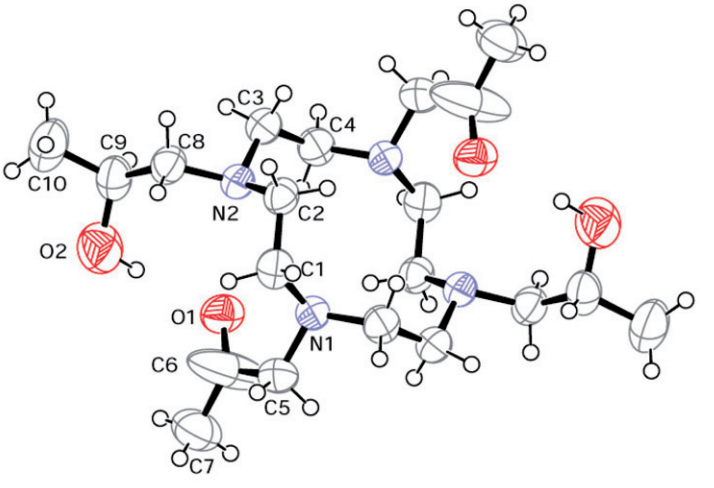

L^4

Figure 5. ORTEP drawing of 1,4,8,11-(2-hydroxypropyl)cyclam, L^3 and 1,4,7,10-(2-hydroxypropyl) cyclen, L^4.

the macrocycle plane while the others fold under the plane which means that the cyclam ring with tetra-pendant arm is reasonably flexible allowing complexation with many different metal ions in many oxidation states, as well as copper(II). Inclusion of tetra-(2-hydroxpropyl) pendants provide strong binding groups which increase the rate of reaction six times in $L^1 \rightarrow L^3$ and 28 times in $L^2 \rightarrow L^4$ while causing decrease in complex stability.

3.2. *Spectrophotometric titration*

The log K_{ML} and K_{MLH} values together with their uncertainties are given in table 3. The stability constant of CuL^3 was also studied by potentiometric method and K_{ML} was 27.2 [31]. The stability constants of the copper(II) complexes with L^1, L^2, L^3, and L^4 increase in the sequence $Cu(L^1) > Cu(L^2) > Cu(L^3) > Cu(L^4)$. There are many factors which may affect the complex formation between metal ions and tetraazamacrocycles, such as variation of basicity of donor, size of metal ions, cavity of macrocycles and steric affects. It has been observed that with an increase in the macrocyclic cavity, there is an increase in complex stability for Cu(II). As the macrocyclic cavity increases, the affinity for Cu(II) increases. This may result from Cu(II) often being in the macrocyclic cavity. Macrocycles have pre-arranged set of donors, thus lowering the entropic barrier of formation and providing a more stable complex in comparison to their acyclic analogues. Due to the flexible nature of the macrocyclic ring, complexes of cyclam derivatives tend to adopt a range of configurational geometries in both the solid state and solution. In order to fully envelope an octahedral metal, L^3 and L^4 have pendant arms with additional donors. The pendant arms serve several purposes, filling first coordination sphere of the metal, balancing the positive charge of the metal and acting as site for further chemistry.

4. Conclusions

The discussion in this article is centered on different chemical behavior exhibited by tetraazamacrocycles that differ in cavity size and appended pendant groups. Pendant groups and cavity size of the macrocycles affect the nature of its metal ion coordination. It is possible to design macrocycles that fit better with one metal ion than the others, making it possible for macrocycles to selectively bind one metal over another. This provides the opportunity to develop specific metal ion sensors by manipulating the structure of macrocycles.

Supplementary material

Supplementary data are available from the Cambridge Crystallographic Data Centre on request, quoting the deposit numbers 772017 for L^3 and 772016 for L^4.

Acknowledgments

Financial support is received from the Scientific and Technological Research Council of Turkeys research program 1001. Grant for 104T389 is gratefully acknowledged.

References

[1] R.R. Fenton, L.F. Lindoy, R.C. Luckay, F.R. Turville, G. Wei. *Aust. J. Chem.*, **54**, 59 (2002).
[2] D.B. Karybut, P. Gluzinski, J. Kajewiski, A. Kremme, A.J. Misnev. *Eur. J. Inorg. Chem.*, 263 (1999).
[3] P.J. Davies, K.P. Wainwright. *Inorg. Chim. Acta.*, **294**, 103 (1999).
[4] G.M. Freeman, E.K. Barefield, D.G. Van Derveer. *Inorg. Chem.*, **23**, 3092 (1984).
[5] D. Odom, C.J. Gramer, V.G. Young Jr, S.A. Hilderbrand, S.E. Sherman. *Inorg. Chim. Acta*, **297**, 404 (2000).
[6] R.R. Effendy, L.F. Lindoy, J.R. Price, B.W. Skelton, T. Strixner, G. Wei, A.H. White. *J. Inclusion Phenom. Macrocyclic Chem.*, **41**, 185 (2001).
[7] R.D. Hancock. *Acc. Chem. Res.*, **23**, 253 (1990).
[8] S. Sreedaran, K.S. Bharathi, A.K. Rahiman, R. Prabu, R. Jegadeesh, N. Raaman, V. Narayanan. *J. Coord. Chem.*, **62**, 3073 (2009).
[9] T. Gunnlaugsson, J.P. Leonard. *Chem. Commun.*, 3144 (2005).
[10] J.C.G. Bunzli, C. Piguet. *Chem. Soc. Rev.*, **34**, 1048 (2005).
[11] E. Kimura, T. Koike, M. Takahashi. *J. Chem. Soc., Chem. Commun.*, 385 (1985).
[12] K. Warncke, A.S. Utada. *J. Am. Chem. Soc.*, **123**, 8564 (2001).
[13] X.Y. Liang, P.J. Sadler. *Chem. Soc. Rev.*, **33**, 246 (2004).
[14] S.V. Smith. *J. Inorg. Biochem.*, **98**, 1874 (2004).
[15] R.I. Haines, D.R. Hutchings. *Can. J. Chem.*, **81**, 186 (2003).
[16] R.I. Haines, R. Baldwin. *Transition Met. Chem.*, **27**, 284 (2002).
[17] E. Kimura. *Tetrahedron*, **30**, 6175 (1992).
[18] K.P. Wainwright. *Adv. Inorg. Chem.*, **52**, 293 (2001).
[19] D.E. Reichert, J. Lewis, C.J. Anderson. *Coord. Chem. Rev.*, **184**, 3 (1999).
[20] S.J. Paisley, P.J. Sadler. *Chem. Commun.*, 3306 (2004).
[21] C.J. Anderson, M.J. Welch. *Chem. Rev.*, **99**, 2219 (1999).
[22] M. Ramli, S.V. Smith, L.F. Lindoy. *Bioconjugate Chem.*, **20**, 868 (2009).
[23] F. Liang, S.H. Wan, Z. Li, X.Q. Xiang, L. Young, X. Zhou, C.T. Wu. *Curr. Med. Chem.*, **13**, 711 (2006).
[24] J.W. Sibert, A.H. Carry, J.G. Carry. *J. Chem. Soc., Chem. Commun.*, 154 (2002).
[25] J.N. Illey, R. Moreira, E. Rosa. *J. Chem. Soc., Perkin Trans.*, **2**, 1503 (1987).
[26] J.C. Igwe, A.A. Abia. *Int. J. Phys. Sci.*, **2**, 119 (2007).
[27] CrystalClear: Rigaku Corporation (1999). Crystal Clear Software User's Guide, Molecular Structure Corporation, J.W. Pflugrath. *Acta Cryst. D*, **55**, 1718 (1999).
[28] SIR92: A. Altomare, G. Cascarano, C. Giacovazzo, A. Guagliardi, M. Burla, G. Polidori, M. Camalli. *J. Appl. Cryst.*, **27**, 435 (1994).
[29] DIRDIF99: P.T Beurskens, G. Admiraal, G. Beurskens, W.P. Bosman, R. de Gelder, R. Israel, J.M.M. Smits. The DIRDIF-99 program system, Technical Report of the Crystallography Laboratory, University of Nijmegen, The Netherlands (1999).
[30] J.R. Roper, H. Elias. *Inorg. Chem.*, **31**, 1202 (1992).
[31] M. Kodama, E. Kimura. *J. Chem. Soc., Dalton Trans.*, 1473 (1977).